Control
and Cybernetics
VOL. 19 (1990) No. 3–4

Shape Memory Alloys: Mathematical Models for a Class of First Order Solid–Solid Phase Transitions in Metals

by

JÜRGEN SPREKELS [1]

Fachbereich 10 der
Universität–GH Essen,
Postfach 10 37 64,
D 4300 Essen 1,
Germany.

In this paper we give an overview of some recently developed mathematical models to describe the phenomenology of the so–called *shape memory alloys.*

1. Introduction

Shape memory alloys (like *Cu Zn, Cu Sn, Au Cu Zn , Ag Cd, Ti Ni*, to name only a few) are metallic alloys characterized by a strong dependence of their load–deformation (P–D) diagrams on temperature (see Fig. 1). At low temperatures, such an alloy behaves like a plastic body with virginal elastic curve, a yield limit, creep and residual deformation; at high temperature the behaviour is pseudoelastic with two symmetric hysteresis loops.

[1] Partially supported by DFG, SPP "Anwendungsbezogene Optimierung und Steuerung".

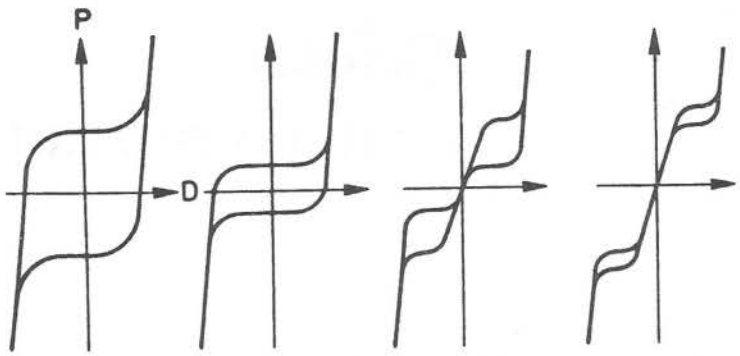

Figure 1. Typical load–deformation curves in shape memory alloys, with temperature increasing from left to right.

If an initially undeformed sample of such a material is at low temperature loaded above the yield limit, a later unloading results in a residual deformation; heating of the deformed sample forces it to creep back to its original (undeformed) state. This so–called *shape memory effect*, which has been exploited in a number of technological applications, is due to first–order phase transitions between different equilibrium configurations of the metallic lattice, termed *austenite* and *martensite*. The highly symmetric austenite is the high temperature phase, while the martensitic variants prevail at low temperatures. In three space dimensions, there exist 24 crystallographically equivalent martensites, resulting from shear deformations of the austenitic configuration. In this paper, we confine ourselves to only one space dimension. Then there are only two martensitic variants, termed *martensitic twins*, which we denote by M_+ and M_-, respectively. The austenitic phase is denoted by A. The corresponding basic lattice elements are depicted in Fig. 2.

The body is then modelled as a stack of layers, each one consisting of such lattice particles. In the following drawing, a load–deformation cycle with shape memory is depicted for a sample which is originally, at low temperature, in the martensitic phase with alternating layers (Fig. 3a). If a load P is applied, we have at first an elastic behaviour (Fig. 3b); once the yield limit is exceeded, the whole body is transformed into one martensitic twin (Fig. 3c), accompanied by a big increase of the total deformation. Unloading then results in a residual deformation (Fig. 3d). Upon heating, the austenitic phase is attained, and the

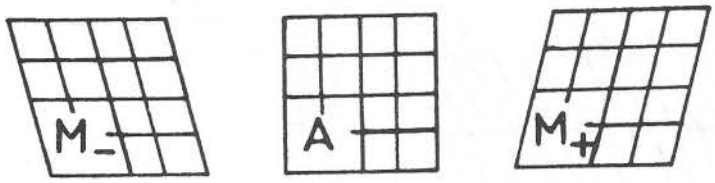

Figure 2. Basic lattice elements.

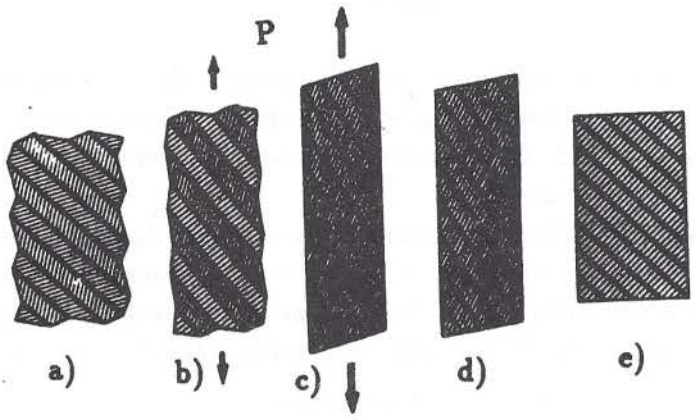

Figure 3. Load–deformation cycle with shape memory.

original shape is recovered (Fig. 3e).

In a series of papers (cf., [2,3,5,28,30,31]), Müller and his co–workers have proposed a structural model based on these observations. Their approach, based on statistical mechanics, models the dynamics of the overall deformation and temperature and ultimately results in a system of ordinary differential equations reflecting rate balances; spatial effects do not show up in the model. Since in this paper we want to focus on models including spatial effects, we do not give a discussion of this approach, here, and we may refer to the above mentioned papers.

In a real crystal, there are always lattice defects leading to a spatially varying shear stress. As a consequence, also the temperature field is nonuniform, and since the equilibrium phase transition temperature depends on the shear stress,

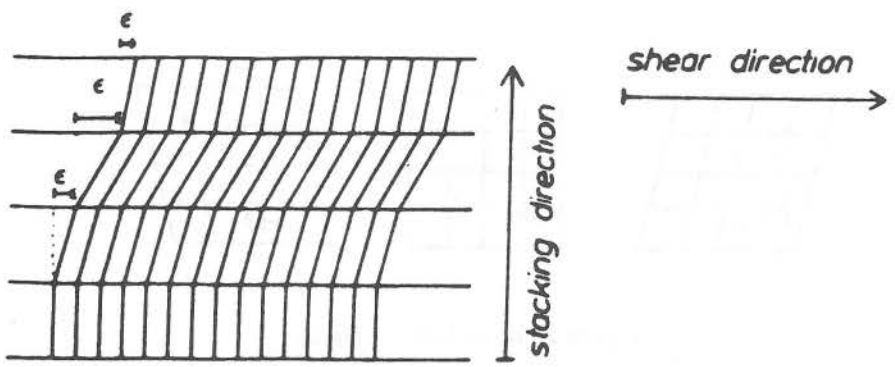

Figure 4.

it will vary within the crystal, as well. Furthermore, phase boundaries carry interfacial energies, so that the local effects of changes of the lattice curvature should not be neglected. It thus makes much sense to consider models which take spatial effects into account.

The dynamics of thermomechanical processes in a one–dimensional solid are governed by the conservation laws of linear momentum, energy and mass. As there is only a very small volume change observed in actual experiments, the latter may be ignored for the materials under consideration; the two others read

$$\rho u_{tt} - \sigma_x + \mu_{xx} = f, \qquad \rho e_t + q_x - \sigma \epsilon_t - \mu \epsilon_{xt} = g. \tag{1.1}$$

Here, the involved physical quantities have the following meaning: ρ – (constant) mass density, u – displacement, σ – shear stress, μ – couple stress, f – distributed loads, e – specific internal energy, q – heat flux, $\epsilon\,(= u_x)$ – (linearized) shear strain, g – density of heat sources or sinks. Since the body is modelled as a stack of layers , and since the deformation results from shear , the displacement u is taken in the direction of the shear, i.e., orthogonal to the stacking direction (cf., Falk [13–17,19]); in Fig. 4 a typical configuration is depicted. The couple stress accounts for local curvature effects.

In addition to the global balance laws, the mathematical model has to comply with the second princple of thermodynamics, given by the *Clausius – Duhem* – inequality

$$\rho s_t \geq -\left(\frac{q}{\theta}\right)_x + \frac{g}{\theta}, \tag{1.2}$$

where s is the specific entropy and θ stands for the absolute (Kelvin) temperature.

In (1.1), the quantities u, σ, μ, e, q are unknown; the number of unknowns must be reduced. A typical method is to construct an expression for the specific free (Helmholtz) energy $F = F(\epsilon, \epsilon_x, \theta, \vec{z})$, where the vector $\vec{z} = (z_1, ..., z_M)$ stands for possible internal variables of the model, such as phase fractions. Next we use the thermodynamical relations

$$s = -\frac{\partial F}{\partial \theta}, \qquad e = F + \theta\, s = F - \theta \frac{\partial F}{\partial \theta}, \tag{1.3}$$

and we assume a form for the heat flux q, normally *Fourier's law*

$$q = -\kappa\, \theta_x, \tag{1.4}$$

where κ is the heat conductivity. Next, constitutive equations relating σ and μ to F have to be introduced. In view of (1.1) and (1.4), the Clausius–Duhem inequality (1.2) postulates that the inequality

$$\rho \left(\frac{\partial F}{\partial \epsilon}\, \epsilon_t + \frac{\partial F}{\partial \epsilon_x}\, \epsilon_{xt} + \sum_{i=1}^{M} \frac{\partial F}{\partial z_i}\, z_{i,t} \right) \leq \sigma\, \epsilon_t + \mu\, \epsilon_{xt} \tag{1.5}$$

be satisfied. It is customary to assume that the behaviour is non–dissipative with respect to the mechanical quantities, i.e., one takes

$$\sigma = \rho \frac{\partial F}{\partial \epsilon}, \qquad \mu = \rho \frac{\partial F}{\partial \epsilon_x}, \tag{1.6}$$

so that (1.5) reduces to

$$\rho \sum_{i=1}^{M} \frac{\partial F}{\partial z_i}\, z_{i,t} \leq 0. \tag{1.7}$$

To complete the model, a law reflecting the evolution of the internal variables, as well as appropriate initial and boundary conditions, have to be prescribed.

In the sequel, we give two different approaches along these lines : In Section 2, a Landau–Ginzburg theory without internal variables due to Falk [13–17,19] is described, while Section 3 brings a discussion of Frémond's [21,22] model which uses phase fractions and a non–differentiable free energy. Section 4 brings some numerical results. Some concluding remarks are given in Section 5. For the reader's convenience, we have included a number of related papers in the list of references that are not explicitly referred to during the course of the paper.

2. Landau–Ginzburg Theory : Falk's Model

In a series of papers (cf., [13–17,19]), Falk gave a one–dimensional model in the framework of Landau's theory of phase transitions. In view of the close analogy between the load–deformation curves in shape memory alloys and the polarization–field curves in ferroelectrics, he used the shear strain as the *order parameter* in Landau's theory and assumed the free energy density $\tilde{F} = \rho F$ in the Landau–Devonshire form

$$\tilde{F}(\epsilon, \epsilon_x, \theta) = \tilde{F}_0(\theta) + \gamma(\theta - \theta_1)\epsilon^2 - \beta\epsilon^4 + \alpha\epsilon^6 + \delta\epsilon_x^2, \tag{2.1}$$

where $\alpha, \beta, \gamma, \delta$ are constants characterizing the actual material and θ_1 is a critical temperature. A typical form for $\tilde{F}_0$ is

$$\tilde{F}_0(\theta) = -c_e\,\theta\,\log(\theta/\tilde{\theta}) + c_e\,\theta + C, \tag{2.2}$$

where c_e is the specific heat, $\tilde{\theta}$ a temperature depending on the material, and C a constant. Note that internal variables do not show up. Fig. 5 brings a plot of $\tilde{F}(\cdot, 0, \theta)$ (above) and $\sigma = \frac{\partial \tilde{F}}{\partial \epsilon}(\cdot, 0, \theta)$ (below) for different temperatures.

In the physical interpretation, the symmetric lateral minima of $\tilde{F}$ correspond to the martensitic twins M_- and M_+, while the central minimum represents the austenite. Non–convex branches of $\tilde{F}$ (or, equivalently, branches where the stress–strain relation is decreasing) correspond to unstable states; consequently, a hysteresis whose maximal size is indicated by the dashed lines may occur. The temperatures cited in the plot have the following meanings:
Below θ_1, there is no central minimum, and austenite is unstable. Between θ_1 and $\theta_2 = \theta_1 + \frac{\beta^2}{3\alpha\gamma}$, all three phases may coexist, where, at $\theta_C = \theta_1 + \frac{\beta^2}{4\alpha\gamma}$, the three minima have equal depth. Above θ_2, only the central minimum exists, and for $\theta > \theta_3 = \theta_1 + \frac{3\beta^2}{5\alpha\gamma}$, the free energy is a convex function so that no hysteresis may occur.

The similarity between the σ–ϵ curves depicted in Fig. 5 and the load–deformation curves of Fig. 1 is obvious; hence with a free energy of the form (2.1) many of the phenomena observed in shape memory alloys can be explained (cf., the detailed discussion in [14,15]). In addition, no internal variables occur in the model, so that (1.4) and (1.6) imply the validity of the second principle of thermodynamics. However, in some aspects the Landau – Ginzburg model does not match the experimental observations; we shall come back to this point in Section 5.

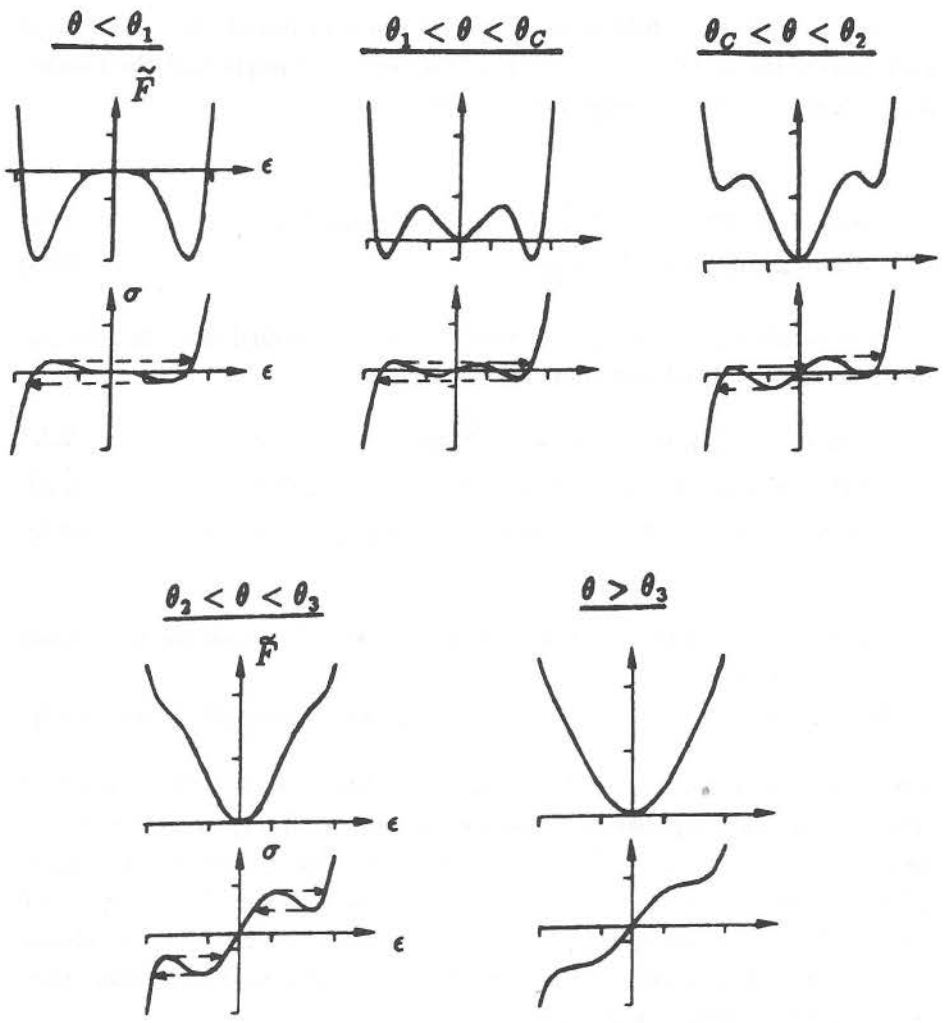

Figure 5. Free energy and stress–strain relations in the Landau–Devonshire theory.

We now derive the field equations for the present model. For a sample of unit length, the identities (1.3), (1.4), (1.6) and (2.1) imply that the balance laws of momentum and energy take the form

$$\rho u_{tt} - \left(2\gamma(\theta - \theta_1) - 4\beta u_x^3 + 6\alpha u_x^5\right)_x + 2\delta u_{xxxx} = f, \tag{2.3a}$$

$$c_e \theta_t - 2\gamma\theta u_x u_{xt} - \kappa\theta_{xx} = g, \tag{2.3b}$$

to be satisfied in $(0,1) \times (0,T)$, where $T > 0$ is some final time. In addition, we prescribe the initial and boundary conditions

$$u(x,0) = u_0(x),\ u_t(x,0) = u_1(x),\ \theta(x,0) = \theta_0(x), \quad x \in [0,1], \tag{2.3c}$$

$$u(0,t) = u_{xx}(0,t) = 0 = u(1,t) = u_{xx}(1,t), \quad t \in [0,T], \tag{2.3d}$$

$$\theta_x(0,t) = 0, \quad -\kappa\,\theta_x(1,t) = \bar{\kappa}\,(\theta(1,t) - \theta_\Gamma(t)), \quad t \in [0,T], \tag{2.3e}$$

where $\bar{\kappa} > 0$ is a heat exchange coefficient, and θ_Γ stands for the outside temperature at $x = 1$.

The following result has been proved in Sprekels–Zheng [40, Theorem 2.1] :

Theorem 2.1 *Suppose* $u_0 \in H^5(0,1)$, $u_1 \in H^3(0,1)$, $\theta_0 \in H^4(0,1)$ *and* $\theta_\Gamma \in H^2(0,T)$ *satisfy compatibility conditions of sufficiently high order at* $x = 0$ *and* $x = 1$, *and assume that* $f, g \in H^1(0,T;H^1(0,1))$ *satisfy* $f_{tt}, g_{xx} \in L^2(0,T;L^2(0,1))$. *Furthermore, let* $g(x,t) \geq 0$, *on* $[0,1] \times [0,T]$, *and* $\theta_\Gamma(t) > 0$, *on* $[0,T]$. *Then the system (2.3a–e) has a unique global classical solution* (u,θ) *where* θ *stays positive throughout. Moreover, all partial derivatives entering (2.3a,b) are Hölder continuous.*

Remarks:

1. Under the hypotheses of Theorem 2.1, the mapping $(f,g,\theta_\Gamma) \mapsto (u,\theta)$ is directionally differentiable. This result can be used to derive necessary conditions of optimality for the solution of related optimal control problems using (f,g,θ_Γ) as control variables. For a detailed discussion we refer to [6].

2. Theorem 2.1 extends earlier results of Sprekels [37,38] and Zheng [42], where stronger growth assumptions for the dependence of $\tilde{F}$ with respect to θ had to be imposed.

3. The above model does not include possible viscous effects in the material. If viscous stresses are present, the global balance laws (2.3a,b) have to be modified. For the case $\delta = 0$ (no couple stresses) a related existence result has been proved by Dafermos [10]. We also refer to [26,33,35], where the results established in these papers are of questionable physical value since a form for the heat flux q was used which does not comply with (1.2).

4. A convergent algorithm for the approximate solution of system (2.3a–e) has been developed in [34]; for details we refer to Section 4.

5. The Landau–Ginzburg model considered in this section is only one– dimensional. A three–dimensional version has been introduced in Falk–Konopka [20]. A mathematical analysis of the latter model has not yet been carried out.

6. Other boundary conditions than (2.3d) can also be considered.

7. In [16,23] the possible steady state solutions of the model have been investigated.

3. The Use of Convex Analysis: Frémond's Model

The Landau–Ginzburg model presented in Section 2 uses the same expression of the free energy for all phases. In contrast to that, the approach used by Frémond [21,22] is based on the assumption that to each phase there corresponds an associated free energy; the total free energy then results from averaging over the phases. Although Frémond's original model is three–dimensional, we restrict ourselves to the simplest one–dimensional case. To this end, we associate with the phases M_+, M_-, A the phase fractions z_1, z_2, z_3 , as well as the (specific) free energies F_1, F_2, F_3 , in that order. We assume the F_i in the form

$$F_1(\epsilon, \epsilon_x, \theta) = F_0(\theta) + \frac{K_1}{2}\epsilon^2 - \alpha(\theta)\epsilon + K_2\,\epsilon_x^2, \tag{3.1a}$$

$$F_2(\epsilon, \epsilon_x, \theta) = F_0(\theta) + \frac{K_1}{2}\epsilon^2 + \alpha(\theta)\epsilon + K_2\,\epsilon_x^2, \tag{3.1b}$$

$$F_3(\epsilon, \epsilon_x, \theta) = F_0(\theta) + \frac{K_1}{2}\epsilon^2 - \frac{L}{\theta_1}(\theta - \theta_1) + K_2\,\epsilon_x^2, \tag{3.1c}$$

where $F_0 = \rho^{-1}\,\tilde{F}_0$ with $\tilde{F}_0$ given by (2.2). K_1, K_2 denote positive physical constants, and θ_1 has the same meaning as in the previous section. L is the (specific) latent heat of the austenite–martensite phase change at the temperature θ_1, while α denotes some (sufficiently smooth) function with the property that for some $\theta_2 > \theta_1$ there holds

$$\alpha(\theta) > 0\,, \text{ for } 0 < \theta < \theta_2, \quad \alpha(\theta) = 0\,, \text{ for } \theta \geq \theta_2. \tag{3.2}$$

Assuming the additivity of the phase free energies, we obtain for the total specific energy

$$F(\epsilon, \epsilon_x, \theta, z_1, z_2, z_3) = \sum_{i=1}^{3} z_i\, F_i(\epsilon, \epsilon_x, \theta) + K_3\,\theta\,\tilde{I}(z_1, z_2, z_3), \tag{3.3}$$

where $K_3 > 0$ is some constant, while $\tilde{I}$ denotes the indicator function of the set

$$M = \{\vec{z} = (z_1, z_2, z_3) \in \mathbb{R}^3 \,|\, 0 \leq z_1, z_2, z_3 \leq 1\,,\; z_1 + z_2 + z_3 = 1\}. \tag{3.4}$$

Recall that $\tilde{I}(\vec{z}) = 0$, for $\vec{z} \in M$, and $= +\infty$, otherwise. The term $K_3\,\theta\,\tilde{I}$ may be interpreted as a mixture free energy; it forces the phase fractions to take on physically meaningful values. Elimination of z_3 leads to independent variables, and the free energy, still denoted F, takes the form

$$\begin{aligned} F(\epsilon, \epsilon_x, \theta, z_1, z_2) &= F_0(\theta) + \frac{K_1}{2}\epsilon^2 + K_2\,\epsilon_x^2 + (z_2 - z_1)\alpha(\theta)\epsilon \\ &+ \frac{L}{\theta_1}(\theta - \theta_1)(z_1 + z_2 - 1) + K_3\,\theta\,I(z_1, z_2), \end{aligned} \tag{3.5}$$

where I denotes the indicator function of the plane triangle

$$\mathcal{T} = \{(z_1, z_2) \in \mathbb{R}^2 \,|\, 0 \leq z_1, z_2 \leq 1\,,\; z_1 + z_2 \leq 1\}. \tag{3.6}$$

From (1.6) we obtain

$$\sigma = \rho\,(K_1\,\epsilon + (z_2 - z_1)\,\alpha(\theta))\,, \quad \mu = 2\,\rho\,K_2\,\epsilon_x. \tag{3.7}$$

Next consider (1.7). For a differentiable F a natural postulate would be

$$-k\,\frac{\partial z_i}{\partial t} = \frac{\partial F}{\partial z_i}(\epsilon, \epsilon_x, \theta, z_1, z_2), \quad i = 1, 2, \tag{3.8}$$

with some $k \geq 0$. For $k > 0$ the system is dissipative while for $k = 0$ it is not. In our case F has no classical derivatives with respect to the z_i. However, F is convex in $\vec{z} = (z_1, z_2)$, and we thus may replace (3.8) by

$$-k\,\vec{z}_t \;\in\; \partial_{\vec{z}} F(\epsilon, \epsilon_x, \theta, z_1, z_2), \tag{3.9}$$

where $\partial_{\vec{z}} F(\epsilon, \epsilon_x, \theta, z_1, z_2)$ denotes the subdifferential of F at $(\epsilon, \epsilon_x, \theta, z_1, z_2)$ with respect to (z_1, z_2). By definition, this is the set of all $\xi \in \mathbb{R}^2$ satisfying the variational inequality

$$\begin{aligned} &F(\epsilon, \epsilon_x, \theta, v_1, v_2) \\ &-F(\epsilon, \epsilon_x, \theta, z_1, z_2) \geq \vec{\xi} \cdot (\vec{v} - \vec{z}), \quad \forall\, \vec{v} = (v_1, v_2) \in \mathbb{R}^2. \end{aligned} \tag{3.10}$$

A simple calculation shows that

$$\begin{aligned} &\partial_{\vec{z}} F(\epsilon, \epsilon_x, \theta, z_1, z_2) \\ &= \alpha(\theta)\,\epsilon \begin{pmatrix} -1 \\ 1 \end{pmatrix} + \frac{L}{\theta_1}(\theta - \theta_1) \begin{pmatrix} 1 \\ 1 \end{pmatrix} + K_3\,\theta\,\partial I(\vec{z}), \end{aligned} \tag{3.11}$$

where

$$\begin{aligned} \partial I(\vec{z}) &= \{\vec{0}\}\ , \text{ if } \vec{z} \in \operatorname{int} \mathcal{T}\ , \\ &= \emptyset\ , \text{ if } \vec{z} \notin \mathcal{T}\ , \\ &= \mathcal{N}(\vec{z})\ , \text{ if } \vec{z} \in \partial \mathcal{T}, \end{aligned} \tag{3.12}$$

with $\mathcal{N}(\vec{z}) = \{\vec{\xi} \in \mathbb{R}^2 \,|\, 0 \geq \vec{\xi} \cdot (\vec{v} - \vec{z})\ ,\ \forall\, \vec{v} \in \mathcal{T}\}$ denoting the set of outer normals to $\mathcal{T}$ at $\vec{z} \in \partial \mathcal{T}$. In Fig. 6 the outer normals are depicted.

Next we examine the resulting stress–strain relations in the non–dissipative case $k = 0$. We have $\sigma = \rho\,(K_1\,\epsilon + (z_2 - z_1)\,\alpha(\theta))$, and the relation $\vec{0} \in \partial_{\vec{z}} F(\epsilon, \epsilon_x, \theta, z_1, z_2)$ takes in view of (3.11), (3.12) the explicit form

$$\alpha(\theta)\,\epsilon\,(v_2 - v_1 - z_2 + z_1) + \frac{L}{\theta_1}(\theta - \theta_1)\,(v_1 + v_2 - z_1 - z_2) \geq 0\ , \quad \forall\, \vec{v} \in \mathcal{T}\ . \tag{3.13}$$

Consider the low temperature range where $\theta < \theta_1$. Then $\alpha(\theta) > 0$ and $\theta - \theta_1 < 0$. Let $\epsilon = 0$. Choosing $(v_1, v_2) \in \mathcal{T}$ with $v_1 + v_2 = 1$, we deduce from (3.13) that $z_1 + z_2 = 1$. We thus have a mixture of martensites, and σ may take on any value in the interval $[-\rho\,\alpha(\theta), +\rho\,\alpha(\theta)]$. Next consider the case $\epsilon < 0$. Then we choose $\vec{v} = (0, 1)$ to obtain that the inequality

$$\alpha(\theta)\,\epsilon\,(1 - z_2 + z_1) + \frac{L}{\theta_1}(\theta - \theta_1)\,(1 - z_1 - z_2) \geq 0 \tag{3.14}$$

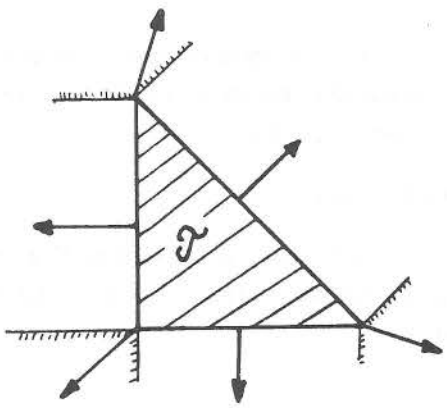

Figure 6. Normals to the triangle $\mathcal{T}$.

must hold, whence we derive that $z_1 = 0\,, z_2 = 1$. Consequently, we have pure M_-, and $\sigma = \rho\,(K_1\,\epsilon + \alpha(\theta))$, for $\epsilon < 0$. For $\epsilon > 0$, an analogous argument shows that $z_1 = 1$, $z_2 = 0$, so that we have pure M_+, and $\sigma = \rho\,(K_1\,\epsilon - \alpha(\theta))$. The temperature ranges $\theta_1 < \theta < \theta_2$ and $\theta > \theta_2$, respectively, can be treated similarly. We refer to [8,21,22]. Fig. 7 gives an impression of the resulting stress–strain relations.

Obviously also the stress–strain relations depicted in Fig. 7 qualitatively resemble the load–deformation curves of Fig. 1; in particular, a hysteresis may occur whose maximal width is indicated by the dashed lines. Hence also Frémond's model can give a qualitative explanation of many of the observed phenomena. We now derive the field equations, again for a sample of unit length. The balance laws of energy and momentum take the form

$$\rho\,(u_{tt} - K_1\,u_{xx} - (\alpha(\theta)(z_2 - z_1))_x + 2\,K_2\,u_{xxxx}) = f, \tag{3.15a}$$

$$\begin{aligned}&(c_e - \rho\,\theta\alpha''(\theta)\,u_x\,(z_2 - z_1))\theta_t - \rho\,\theta\alpha'(\theta)\,(z_2 - z_1)u_{xt} - \rho\,L\,(z_1 + z_2)_t\\ &+\rho\,(\alpha(\theta) - \theta\alpha'(\theta))\,u_x\,(z_2 - z_1)_t - \kappa\,\theta_{xx} = g,\end{aligned} \tag{3.15b}$$

to be satisfied in $(0,1) \times (0,T)$. In addition, from (3.8) and (3.11) we obtain for the evolution of the phase fractions the variational inequality

$$-k\,\vec{z}_t \;\in\; \alpha(\theta)\,u_x \begin{pmatrix} -1 \\ 1 \end{pmatrix} + \frac{L}{\theta_1}\,(\theta - \theta_1) \begin{pmatrix} 1 \\ 1 \end{pmatrix} + K_3\,\theta\,\partial I(\vec{z}), \tag{3.15c}$$

with $\partial I(\vec{z})$ given by (3.12). Here, and in the sequel, we assume that $k > 0$. We add the initial and boundary conditions

$$u(x,0) = u_0(x),\; u_t(x,0) = u_1(x),$$

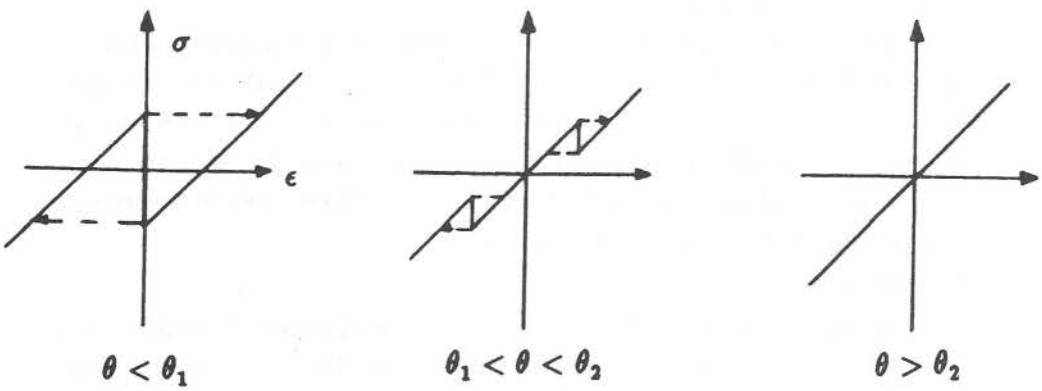

Figure 7. Stress-strain curves at different temperatures with possible hysteresis along the dashed lines.

$$\theta(x,0) = \theta_0(x),\ \vec{z}(x,0) = \vec{z}_0(x), \quad x \in [0,1], \tag{3.15d}$$

$$u(0,t) = u_{xx}(0,t) = u_{xx}(1,t) = 0,$$

$$\sigma(1,t) - \mu_x(1,t) = \ell(t)\,, \quad t \in [0,T]\,, \tag{3.15e}$$

$$\theta_x(0,t) = 0\,, \quad -\kappa\,\theta_x(1,t) = \bar{\kappa}\,(\theta(1,t) - \theta_\Gamma(t))\,, \quad t \in [0,T]\,. \tag{3.15f}$$

Here $\ell(t)$ denotes the external traction at $x = 1$.

Even in the one–dimensional case described here it is an as yet open problem if (3.15a–f) has a solution. However, some global existence and uniqueness results have been proved for the three-dimensional version of (3.15a–f) if simplifications are made. All these results are concerned with the *quasistationary* case where the term $\rho\,u_{tt}$ is discarded; also, in all the works cited below the term $-\rho\,\theta\alpha''(\theta)\,u_x\,(z_2 - z_1)\,\theta_t$ is missing. The latter simplification seems acceptable while the former has a restricted applicability.

The first result was given by Colli–Frémond–Visintin [8] (see also Colli [7], for a generalization). They proved existence of a unique weak solution under the assumption that not only the above mentioned terms are omitted, but also the expressions $-\rho\,\theta\,\alpha'(\theta)\,(z_2 - z_1)\,u_{xt}$ and $\rho\,(\alpha(\theta) - \theta\,\alpha'(\theta))\,u_x\,(z_2 - z_1)_t$. Note that these terms contribute significantly to the exchange of the thermal and mechanical energies. Recently Colli–Sprekels [9] have demonstrated that existence

can still be obtained if the latter of these terms is retained in (3.15b), but they could not prove uniqueness.

Hoffmann–Niezgódka–Zheng [25] made a different simplification. They retained both terms and mollified (3.15c) instead by replacing the left–hand side by the expression $-k\,\vec{z}_t + \Delta\vec{z}$. For sufficiently small $\|\alpha\|_{C^1}$ existence, and in the one–dimensional case also uniqueness, could be proved. However, the introduction of the diffusive term $\Delta\vec{z}$ into (3.15c) is questionable since martensitic transformations are known to be diffusion–free.

Remarks:

8. Numerical simulations for Frémond's model with physically realistic data have apparently not yet been reported in print. Thus at the present stage a statement about the quantitative behaviour of the model is impossible.

9. It would be important to analyze the structure of possible steady–state solutions of (3.15a–f).

4. Numerical Results

In this section we describe an algorithm for the numerical solution of system (2.3a–e) which has been introduced in Niezgódka–Sprekels [34], and we report some numerical results which have been obtained with this algorithm. To this end, we choose $K, N, M \in \mathbb{N}$, and we define

$$F_0(\epsilon,\theta) := \gamma(\theta-\theta_1)\epsilon^2 - \beta\epsilon^4 + \alpha\epsilon^6. \tag{4.1}$$

Moreover, we put $h = \frac{T}{M}$, $t_m^{(M)} = mh$, $0 \le m \le M$, and $x_i^{(N)} = \frac{i}{N}$, $0 \le i \le N$.

Let $Z_K = \mathrm{span}\{z_1,\dots,z_K\}$, where z_j denotes the j–th eigenfunction of the eigenvalue problem $z'''' = \lambda z$, in $(0,1)$, $z(0) = z''(0) = 0 = z(1) = z''(1)$, and denote by Y_N the linear space of linear splines on $[0,1]$ corresponding to the partition $\{x_i^{(N)}\}_{i=0}^N$ of $[0,1]$.

Now let P_K denote the H^4–orthogonal projection onto Z_K, Q_K the H^2–orthogonal projection onto Z_K, and R_N the H^1–orthogonal projection onto Y_N. Furthermore, we introduce the averages

$$f_M^m(x) = \frac{1}{h}\int_{(m-1)h}^{mh} f(x,t)dt\,, \quad g_M^m(x) = \frac{1}{h}\int_{(m-1)h}^{mh} g(x,t)dt\,,$$
$$\theta_{\Gamma,M}^m = \frac{1}{h}\int_{(m-1)h}^{mh} \theta_\Gamma(t)dt. \tag{4.2}$$

We consider the discrete problem

$(\mathbf{D_{M,N,K}})$:

Find $u^m = \sum_{k=1}^K \alpha_k^m z_k$, $\theta^m = \sum_{k=0}^N \beta_k^m y_k^{(N)}$, $1 \le m \le M$, such that

$$\int_0^1 \Big(\rho \frac{u^m - 2u^{m-1} + u^{m-2}}{h^2} \xi + 2\delta u_{xx}^m \xi_{xx} - f_M^m \xi + \xi_x \left(F_0(u_x^m, \theta^{m-1}) - F_0(u_x^{m-1}, \theta^{m-1})\right)/(u_x^m - u_x^{m-1}) \Big) dx = 0, \quad \forall \xi \in Z_K, \tag{4.3a}$$

$$\int_0^1 \Big(c_e \frac{\theta^m - \theta^{m-1}}{h} \eta - \gamma \theta^{m-1} \frac{(u_x^m)^2 - (u_x^{m-1})^2}{h} \eta + \kappa \theta_x^m \eta_x - g_M^m \eta \Big) dx + \bar{\kappa} (\theta^m(1) - \theta_{\Gamma,M}^m) \eta(1) = 0, \quad \forall \eta \in Y_N, \tag{4.3b}$$

$$u^0 = P_K(u_0), \quad \frac{u^0 - u^{-1}}{h} = Q_K(u_1), \quad \theta^0 = R_N(\theta_0). \tag{4.3c}$$

The following result has been proved in [34] :

Theorem 4.1 *Suppose the assumptions of Theorem 2.1 are satisfied and suppose N is sufficiently large. Then there exist constants $\bar{C}_1 > 0$, $\bar{C}_2 > 0$ which do not depend on M,N,K, such that for $\frac{c_e}{6\kappa N^2} < h \le \bar{C}_1$ the discrete problem $(D_{M,N,K})$ has a solution which satisfies*

$$\theta^m(x) \ge 0, \quad \forall x \in [0,1], \quad 0 \le m \le M, \tag{4.4a}$$

$$\max_{0 \le m \le M} \left(\left\| \frac{u^m - u^{m-1}}{h} \right\|^2 + \left\| \frac{u_x^m - u_x^{m-1}}{h} \right\|^2 + \|u_{xxx}^m\|^2 \right) \le \bar{C}_2, \tag{4.4b}$$

$$\max_{0 \le m \le M} (\|\theta_x^m\|^2 + |\theta^m(1)|^2) + \sum_{m=1}^M h \left\| \frac{\theta^m - \theta^{m-1}}{h} \right\|^2 \le \bar{C}_2. \tag{4.4c}$$

It is easy to obtain convergent approximations from Theorem 4.1. To this end, let $\varphi : \mathbb{N} \to \mathbb{N}$ be strictly increasing. We take $N = \varphi(K)$, $M = M(N)$ with $\frac{T}{M} > \frac{c_e}{6\kappa N^2}$, and we choose $K \in \mathbb{N}$ large enough. Denoting the corresponding solutions of $(D_{M,N,K})$ by $\{(u_K^m, \theta_K^m)\}_{m=1}^M$ and introducing the linear–in–time interpolations

$$\begin{aligned} u_K(\cdot,t) &= (Mt - m + 1)\, u_K^m + (m - Mt)\, u_K^{m-1}, \\ \theta_K(\cdot,t) &= (Mt - m + 1)\, \theta_K^m + (m - Mt)\, \theta_K^{m-1}, \\ & \qquad (m-1)h \le t \le mh, \quad m = 1, \dots, M, \end{aligned} \tag{4.5}$$

we obtain that (cf., [34])

$$u_{K,x} \to u_x\,, \quad \theta_K \to \theta\,, \text{ uniformly on } [0,1]\times[0,T]\,. \tag{4.6}$$

The above algorithm has been tested numerically for the alloy $Au_{23}\,Cu_{30}\,Zn_{47}$. For this alloy, the following data have been reported in [16]:
$\alpha = 7.5\times 10^6\,J\,cm^{-3}$, $\beta = 1.5\times 10^5\,J\,cm^{-3}$, $\gamma = 24\,J\,cm^{-3}\,K^{-1}$,
$\delta = 10^{-12}\,J\,cm^{-1}$, $c_e = 2.9\,J\,cm^{-3}\,K^{-1}$, $\theta_1 = 208\,K$, $\kappa = 1.9\,W\,cm^{-1}\,K^{-1}$,
$\rho = 11.1\,g\,cm^{-3}$.

The numerical values of κ, f, u_1 were taken as zero; furthermore, we chose $\theta_0(x) \equiv 200\,K$, $h = 10^{-6}\,sec$, $N = 600$ and $K = 12$. As initial displacement we took the L^2 – orthogonal projection onto Z_K of the function

$$\tilde{u}_0(x) = 0.118\,x\,,\ x \le 0.5\,, \quad \tilde{u}_0 = 0.118\,(1-x)\,,\ x \ge 0.5 \quad [cm]\,. \tag{4.7}$$

This means that initially, at $\theta = 200\,K$, we had an equilibrium configuration consisting of two distinct regions containing different martensites. We applied a distributed heat pulse $g(x,t) = 7.5\times 10^5$ to the system which was switched off after $2.8\times 10^{-3}\,sec$. During that time period, the temperature was raised to more than $300K$, while the crystal lattice was completely transformed into the austenitic configuration. Afterwards, the opposite heat (or rather, cooling) pulse was applied, forcing the system to creep back to its original configuration. We thus observe a temperature–driven shape memory. In Fig. 8 the evolutions of strain (a), temperature (b) and displacement (c) are depicted.

5. Concluding Remarks

10. The previously described models are in good qualitative agreement with many of the experimentally observed phenomena in shape memory alloys. From the quantitative point of view, the Landau–Ginzburg model seems at the present stage to be a little bit better developed than Frémond's model (but this may change soon, of course). Both models account for interfacial energies by using a strain gradient term whose coefficient can only be determined in approximate order. While gradient terms have been introduced repeatedly by physicists in phenomenological theories of other phase transitions, their use is not undisputed. It is thus desirable to avoid the strain gradient terms. As a consequence, the smoothing term u_{xxxx} would not occur in the momentum balance which creates an additional analytic difficulty. A first step in this direction has recently been

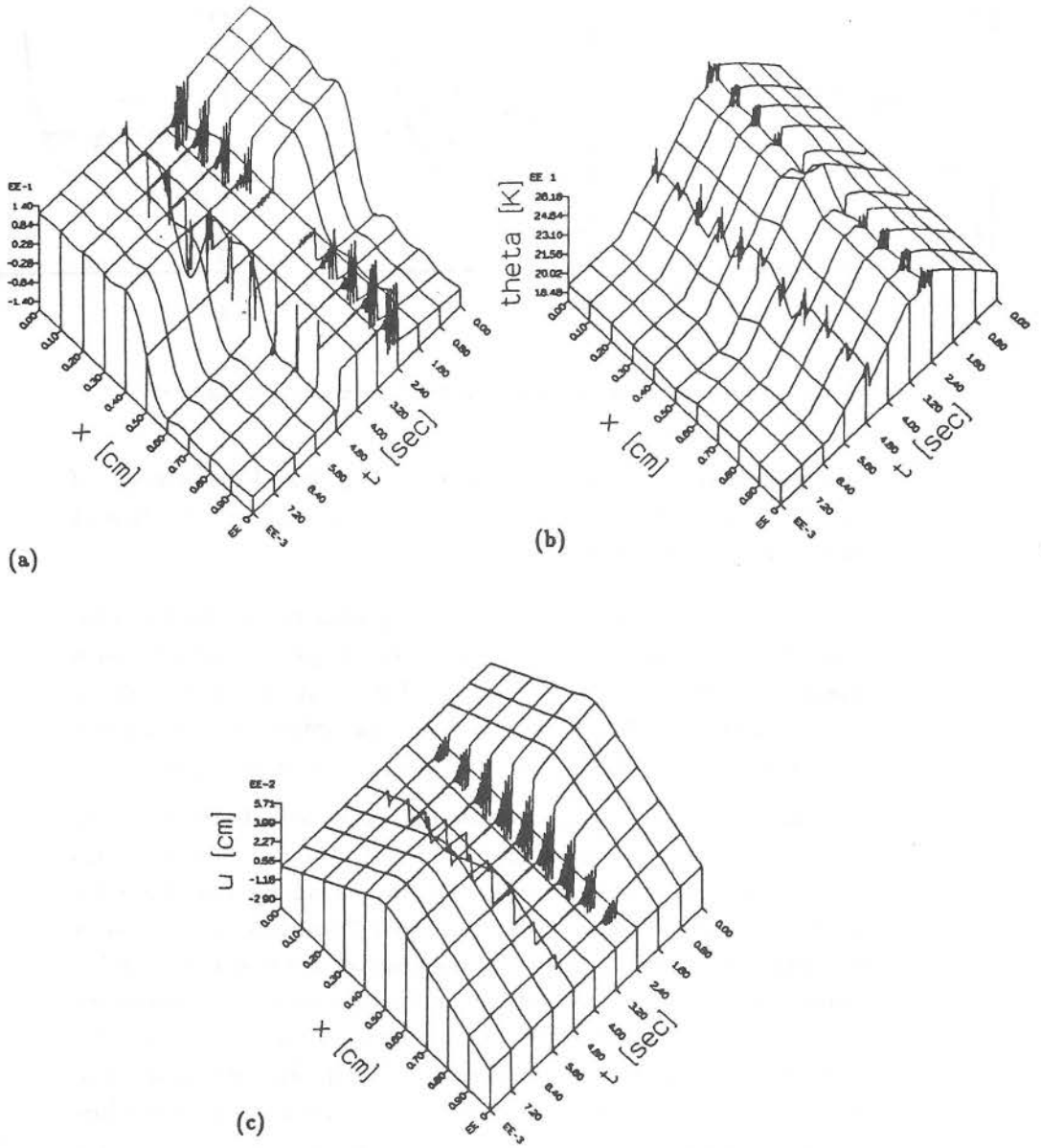

Figure 8. Evolution of strain, temperature and displacement.

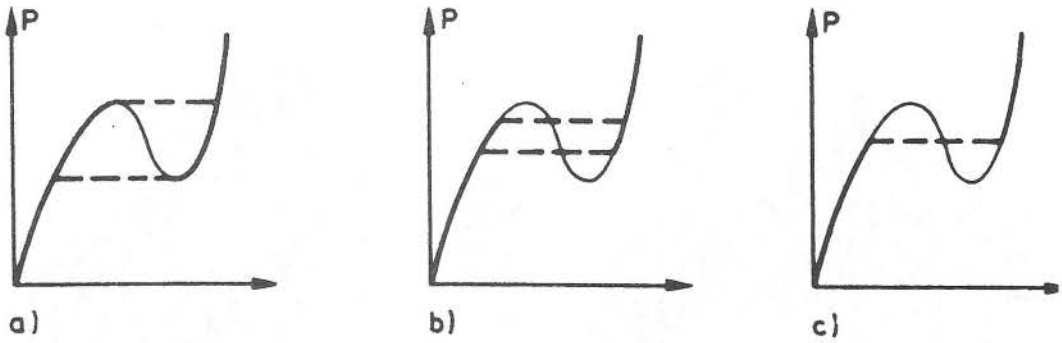

Figure 9. Possible sizes for hysteresis loops in a phase transition.

taken by Bénilan–Blanchard–Ghidouche [4]; they proved the existence of a unique weak solution for the quasistationary Frémond–model without strain gradient term for the *isothermal* case.

11. Both Falk's and Frémond's model can only predict the maximally possible width (in vertical extent) of the hysteresis loops, but not whether a hysteresis actually occurs and if it does, what size it has. Indeed, all the situations depicted in Fig. 9 (maximal width (a), intermediate width (b), zero width ((c), so–called *Maxwell line*) are possible, in principle.

    Furthermore, if the free energy is assumed in the Landau–Devonshire form (2.1), then the vertical width of the loops ought to decrease with temperature in the pseudoelastic range, while experiments indicate that this is not the case (cf., [32]). Finally, neither Falk's nor Frémond's model provides any information about the interior of the loops, except that to each deformation there corresponds an unstable state associated with a point on the downward sloping branch of the load–deformation curve. But states inside the loops are observed in experiments (cf., [32]). Recently, Müller and his co–workers (see [5,29,32]) gave an extension of the Landau–Devonshire approach to answer these questions. Their claim is that the size of the hysteresis depends strongly on the interfacial energies, and they are able to give an interpretation for the states in the interior of the loops. In this new approach the interfacial energies are incorporated as products of phase fractions, and not via strain gradient terms. For details we have to refer to the above mentioned papers. A mathematical analysis of the field

[11] DELAEY, L., CHANDRASEKARAN, M. (EDS.), *International Conference on Martensitic Tranformations, Proceedings.* Les Editions de Physique, Les Ulis 1982.

[12] DELAEY, L., KRISHNAN, R.V., TAS, H., WARLIMONT, H., Thermoelasticity, pseudoelasticity and the memory effects associated with martensitic transformations. *J. Mat. Sci.* **9** (1974), 1521–1555.

[13] FALK, F., Model free energy, mechanics and thermodynamics of shape memory alloys. *Acta Met.* **28** (1980), 1773–1780.

[14] FALK, F., One–dimensional model of shape memory alloys. *Arch. Mech.* **35** (1983), 63–84.

[15] FALK, F., Landau theory and martensitic phase transitions, *J. Phys. C4,* **12** (1982), 3–15.

[16] FALK, F., Ginzburg–Landau theory of static domain walls in shape–memory alloys. *Z. Physik B – Condensed Matter* **51** (1983), 177–185.

[17] FALK, F., Ginzburg–Landau theory and solitary waves in shape–memory alloys. *Z. Physik B – Condensed Matter* **54** (1984), 159–167.

[18] FALK, F., Pseudoelastic stress–strain curves of polycrystalline shape memory alloys calculated from single crystal data. *Int. J. Engng. Sci.* **27** (1989), 277–284.

[19] FALK, F., Elastic phase transitions and nonconvex energy functions. In: *Free Boundary Problems: Theory and Applications, Vol. I* (K.–H. Hoffmann, J. Sprekels, eds.), 45–59, Pitman Research Notes in Math. Ser. No. 185, Longman, 1990.

[20] FALK, F., KONOPKA, P., Three–dimensional Landau theory describing the martensitic phase transformations of shape–memory alloys. *J. Phys.: Condens. Matter* **2** (1990), 61–77.

[21] FRÉMOND, M., Matériaux à mémoire de forme. *C. R. Acad. Sci. Paris, II–304* (1987), 239–244.

[22] FRÉMOND, M., Shape memory alloys. A thermomechanical model. In: *Free Boundary Problems: Theory and Applications, Vol. I* (K.–H. Hoffmann, J.

equations resulting from this model has not yet been performed.

12. A new approach to the phenomena in shape memory alloys which is based on the Preisach model of hysteresis was recently introduced in Huo [27].

References

[1] ACHENBACH, M., A model for an alloy with shape memory. *Int. J. Plasticity* (in print).

[2] ACHENBACH, M., ATANACKOVIC, T., MÜLLER, I., A model for memory alloys in plain strain. *Int. J. Solids and Structures* **22** (1986), 171–193.

[3] ACHENBACH, M., MÜLLER, I., Creep and yield in martensitic transformations. *Ingenieur–Archiv* **53** (1983), 73–83.

[4] BÉNILAN, PH., BLANCHARD, D., GHIDOUCHE, H., On a nonlinear system for shape memory alloys. *Cont. Mech. Thermod.* **1** (1990), 65–76.

[5] BORNERT, M., MÜLLER, I., Temperature dependence of hysteresis in pseudoelasticity. In: *Free Boundary Value Problems* (K.–H. Hoffmann, J. Sprekels, eds.), ISNM 95, 27–35. Birkhäuser Verlag, Basel 1990.

[6] BROKATE, M., SPREKELS, J., Optimal control of thermomechanical phase transitions in shape memory alloys: Necessary conditions of optimality. To appear in *Math. Meth. in the Appl. Sci.*

[7] COLLI, P., An evolution problem related to shape memory alloys. Pubbl. N. 656, IAN CNR, Pavia, 1989.

[8] COLLI, P., FRÉMOND, M., VISINTIN, A., Thermo–mechanical evolution of shape memory alloys. *Quart. Appl. Math.* **158** (1990), 31–47.

[9] COLLI, P., SPREKELS, J., Global existence for a three–dimensional model for the thermo–mechanical evolution of shape memory alloys. Submitted to *European J. Appl. Math.*

[10] DAFERMOS, C.M., Global smooth solutions to the initial boundary value problem for the equations of one–dimensional thermoviscoelasticity. *SIAM J. Math. Anal.* **13** (1982), 397–408.

Sprekels, eds.), 295–306, Pitman Research Notes in Math. Ser. No. 185, Longman, 1990.

[23] FRIEDMAN, A., SPREKELS, J., Steady states of austenitic–martensitic domains in the Ginzburg–Landau theory of shape memory alloys. *Cont. Mech. Thermod.* **2** (1990), 199–213.

[24] HOFFMANN, K.–H., NIEZGÓDKA, M., Mathematical models of dynamical martensitic transformations in shape memory alloys. Submitted to *J. Intelligent Material Syst. Structures.*

[25] HOFFMANN, K.–H., NIEZGÓDKA, M., ZHENG, S., Existence and uniqueness of global solutions to an extended model of the dynamical developments in shape memory alloys. *Nonlinear Analysis TMA* (in print).

[26] HOFFMANN, K.–H., ZHENG, S., Uniqueness for structured phase transitions in shape memory alloys. *Math. Meth. in the Appl. Sci.* **10** (1988), 145–151.

[27] HUO, Y.,A mathematical model for the hysteresis in shape memory alloys. *Cont. Mech. Thermod.* **1** (1989), 283–303.

[28] MÜLLER, I., Pseudoelasticity in shape memory alloys – an extreme case of thermoelasticity. *Proc. Termoelasticitá Finita. Acc. Nat. dei Lincei* **76** (1986), 123–149.

[29] MÜLLER, I., On the size of hysteresis in pseudo–elasticity. *Cont. Mech. Thermod.* **1** (1989).

[30] MÜLLER, I., WILMAŃSKI, K., A model for phase transitions in pseudoelastic bodies. *Il Nuovo Cimento* **57B** (1980), 283–318.

[31] MÜLLER, I., WILMAŃSKI, K., Memory alloys – phenomenology and ersatzmodel. In: *Continuum Models of Discrete Systems IV* (O. Brulin, R.K.T. Hsieh, eds.), 495–509. North–Holland, Amsterdam 1981.

[32] MÜLLER, I., XU, H., On pseudo–elastic hysteresis. Submitted to *Acta Metallurgica.*

[33] NIEZGÓDKA, M., SPREKELS, J., Existence of solutions for a mathematical model of structural phase transitions in shape memory alloys. *Math. Meth. in the Appl. Sci.* **10** (1988), 197–223.

[34] NIEZGÓDKA, M., SPREKELS, J., Convergent numerical approximations of the thermomechanical phase transitions in shape memory alloys. To appear in *Numer. Math.*

[35] NIEZGÓDKA, M., ZHENG SONGMU, SPREKELS, J., Global solutions to a model of structural phase transitions in shape memory alloys. *J. Math. Anal. Appl.* **130** (1988), 39–54.

[36] PERKINS, J. (ED.), *Shape Memory Effects in Alloys.* Plenum Press, New York 1978.

[37] SPREKELS, J., Global existence for thermomechanical processes with non-convex free energies of Ginzburg–Landau form. *J. Math. Anal. Appl.* **141** (1989), 333–348.

[38] SPREKELS, J., Stability and optimal control of thermomechanical processes with non–convex free energies of Ginzburg–Landau type. *Math. Meth. in the Appl. Sci.* **11** (1989), 687–696.

[39] SPREKELS, J., Automatic control of one–dimensional thermomechanical phase transitions. In: *Mathematical Models for Phase Change Problems* (J.F. Rodrigues, ed.), ISNM 88, 89–98. Birkhäuser Verlag, Basel 1989.

[40] SPREKELS, J., ZHENG, S., Global solutions to the equations of a Ginzburg–Landau theory for structural phase transitions in shape memory alloys. *Physica* **D 39** (1989), 39–54.

[41] WILMAŃSKI, K., Propagation of the interface in the stress–induced austenite–martensite transformation. *Ingenieur–Archiv* **53** (1983), 291-301.

[42] ZHENG, S., Global solutions to thermo–mechanical equations with non-convex Landau–Ginzburg free energy. *J. Appl. Math. Phys. (ZAMP)* **40** (1989), 111–127.